Original article

A novel ultralow-loss Sr_2CeO_4 microwave dielectric ceramic and its property modification

Qianlong Dai, Ruzhong Zuo*

Institute of Electro Ceramics & Devices, School of Materials Science and Engineering, Hefei University of Technology, Hefei, 230009, PR China

A B S T R A C T

A new ultralow-loss Sr_2CeO_4 microwave dielectric ceramic was prepared via a conventional solid-state method. The X-ray diffraction and Rietveld refinement results demonstrate that pure-phase Sr_2CeO_4 ceramics belong to the orthorhombic structure with a Pbam space group. Scanning electron microscopy analysis reveals dense and homogeneous microstructure. Optimum microwave dielectric properties of ε_r = 14.8, $Q \times f$ = 172,600 GHz (9.4 GHz) and τ_f = -62 ppm/°C were obtained as it was sintered at 1270 °C for 4 h. In addition, the substitution of a few amount of Ti^{4+} for Ce^{4+} was found to have significant influences on the grain morphology, sintering behavior, phase structure and microwave dielectric properties. Among them, the $Sr_2Ce_{0.65}Ti_{0.35}O_4$ ceramic sintered at 1350 °C for 4 h demonstrates near-zero τ_f of -1.8 ppm/°C, ε_r of 20.7 and $Q \times f$ of 115,550 GHz (8.1 GHz) because of its two-phase structure, showing large application potentials.

1. Introduction

With the rapid development of the microwave communication technology, dielectric ceramics have received wide attention as the A new ultralow-loss Sr_2CeO_4 microwave dielectric ceramic was prepared via a conventional solid-state method. The X-ray diffraction and Rietveld refinement results demonstrate that pure-phase Sr_2CeO_4 ceramics belong to the orthorhombic structure with a Pbam space group. Scanning electron microscopy analysis reveals dense and homogeneous microstructure. Optimum microwave dielectric properties of ε_r = 14.8, $Q \times f$ = 172,600 GHz (9.4 GHz) and τ_f = -62 ppm/°C were obtained as it was sintered at 1270 °C for 4 h. In addition, the substitution of a few amount of Ti^{4+} for Ce^{4+} was found to have significant influences on the grain morphology, sintering behavior, phase structure and microwave dielectric properties. Among them, the $Sr_2Ce_{0.65}Ti_{0.35}O_4$ ceramic sintered at 1350 °C for 4 h demonstrates near-zero τ_f of -1.8 ppm/°C, ε_r of 20.7 and $Q \times f$ of 115,550 GHz (8.1 GHz) because of its two-phase structure, showing large application potentialskey materials for microwave resonators, filters and other passive devices [1,2]. Moreover, the recent progress in Internet of Things (IoT), intelligent transport systems (ITS), the fifth generation mobile communication systems (5 G), etc. has resulted in an increasing need for designs of new microwave dielectric components and dielectric materials with suitable dielectric constant (ε_r), low dielectric loss (high quality factor Q = 1/tanδ) and near-zero temperature coefficient of resonant frequency (τ_f) [3].

Up to now, a great number of low-loss dielectric materials have been widely studied, such as Mg_2SiO_4, $MgAl_2O_4$, $Ba(Mg_{1/3}Ta_{2/3})O_3$, and $Ba(Zn_{1/3}Ta_{2/3})O_3$, but their large negative τ_f have restricted their possible applications in microwave devices. To tune τ_f to near zero, a couple of studies have been focused on various processing methods such as the substitution of B-site ions [4–6] or the adoption of some additives [7]. However, undesired secondary phases and inhomogeneous microstructure might lead to the deterioration in electrical performances because of the chemical reaction of different compositions or phases [8,9].

The orthorhombic Sr_2CeO_4 ceramic has been widely studied as excellent luminescent materials. The blue emitting phosphor was synthesized for the first time using a combinatorial route by Danielson et al. [10]. Sr_2CeO_4 phase seems to possess isomorphic structure of the layered Ruddlesdon-Popper phase Sr_2TiO_4 [11], but belongs to the Sr_2PbO_4-type structure [12,13]. The Sr_2PbO_4-type structure consists of unusual one-dimensional chains of edge-shared CeO_6 octahedra along [001], unlike the two-dimensional edge-shared octahedral TiO_6 planes in Sr_2TiO_4 (space group I4/mmm). As the radius of Ti^{4+} (0.605 Å) is far less than Ce^{4+} (0.87 Å), the solid solubility of Ti^{4+} in B-site is limited. Moreover, the microwave dielectric properties of Sr_2TiO_4 (ε_r = 42, $Q \times f$ = 145,200 GHz, τ_f = + 130 ppm/°C) has been reported by Liu et al. [14]. In this work, a pure-phase Sr_2CeO_4 ceramic was synthesized, with a special focus on its microwave dielectric properties. In addition,

---

* Corresponding author.
  E-mail address: piezolab@hfut.edu.cn (R. Zuo).

a few amount of Ti^{4+} was used to further modify the phase structure and microwave dielectric properties of Sr_2CeO_4 ceramics. The sintering behavior, phase composition, microstructure and microwave dielectric properties of $Sr_2Ce_{1-x}Ti_xO_4$ (0 ≤ x ≤ 0.5) ceramics were studied in detail as well.

2. Experimental

The $Sr_2Ce_{1-x}Ti_xO_4$ (0 ≤ x ≤ 0.5) ceramics were synthesized by a conventional solid-state reaction method using high-purity starting powders of analytic-grade CeO_2, $SrCO_3$ and TiO_2. Stoichiometric amounts of raw powders were weighed according to the formula of $Sr_2Ce_{1-x}Ti_xO_4$. The powder mixtures were first milled with ZrO_2 balls in alcohol for 4 h. After drying, x = 0 and x > 0 powders were calcined at 1100 °C and 1150 °C for 8 h, respectively. The calcined powders were re-milled for 6 h together with 0.5 wt% PVB as a binder. The granulated powders were subsequently pressed into cylinders with dimensions of 10 mm in diameter and 7-8 mm in height. The specimens were first heated at 550 °C in air for 4 h to remove the organic binder, and then sintered at 1230–1430 °C for 4 h.

The bulk densities of the sintered samples were measured by the Archimedes method. The crystalline structure of the sintered samples was determined by an X-ray diffractometer (XRD; D/Max2500 V, Rigaku, Japan). The structural parameters were obtained from the Rietveld refinement of XRD data using the GSAS-EXPGUI program. The microstructure of the sintered samples was observed using a field-emission scanning electron microscope (FE-SEM; SU8020, JEOL, Tokoy, Japan) equipped with an energy dispersive spectrometer (EDS). Microwave dielectric properties were measured using a network analyzer (N5230C; Agilent, Palo Alto, CA) and a temperature chamber (GDW-100, Saiwesi, Changzhou, China). The τ_f values of the samples were measured in the temperature range of 20–80 °C and calculated by the following equation:

$$\tau_f = \frac{f_2 - f_1}{f_1(T_2 - T_1)} \qquad (1)$$

where f_1 and f_2 represent the resonant frequencies at T_1 and T_2, respectively.

3. Results and discussion

Fig. 1(a) presents the XRD pattern of Sr_2CeO_4 ceramics sintered at different temperatures for 4 h. All diffraction peaks can be well indexed according to the Sr_2CeO_4 phase (JCPDS No. 50-0115). As the sintering temperature increases, a small peak near 30° marked by stars can be observed for the sintered ceramic, as shown in Fig. 1(b). This peak
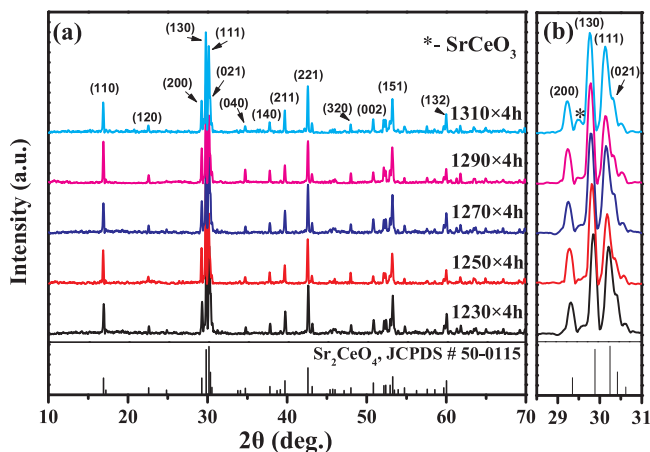
seems to become obvious when the Sr_2CeO_4 sample was sintered at 1310 °C. This secondary phase might be $SrCeO_3$ by comparing its diffraction peaks with the standard pattern (JCPDS No. 83-1156). After the Rietveld refinement, the lattice parameters and reliability factors of R_{wp}, R_P, and χ^2 for all studied samples are listed in Table 1. The refined plot of the sample sintered at 1270 °C was selected as a representative, as shown in Fig. 2. The R_{wp}, R_P, and χ^2 values were found to be in the range of < 9%, < 7% and 1.4–1.7, respectively, indicating that the structural model is valid and the refinement result is reliable. Moreover, the obtained structure parameters are similar to those previously reported [15]. It can be seen that there is no any obvious variation in lattice parameters and cell volumes with increasing firing temperature.

Fig. 3(a)–(c) shows the SEM images of Sr_2CeO_4 ceramics sintered at different temperatures for 4 h. It is evident that Sr_2CeO_4 ceramics can be well sintered within the temperature range of 1270–1310 °C. A relatively uniform microstructure with closely packed polygonal grains was obtained in the sample sintered at 1270 °C. The average grain size slightly increases from ∼ 4 μm to ∼ 7 μm with increasing sintering temperature from 1270 °C to 1310 °C.

Fig. 4 illustrates the relative density and microwave dielectric properties of Sr_2CeO_4 ceramics as a function of sintering temperature. It can be seen that the sample density clearly increases with increasing sintering temperature and reaches its platform approximately at 1270 °C. The decrease of the sample density at 1310 °C might be ascribed to the appearance of the secondary phase and the rapid grain growth (Fig. 3(c)). Above 1270 °C, all samples exhibit high relative densities of > 97%, keeping consistent with the microstructural observation. The same variation trend in ε_r and relative density with sintering temperature indicates that porosity acts as a main influencing factor of dielectric constant. In general, the dielectric loss can be divided into extrinsic loss and intrinsic loss. The extrinsic loss is mainly caused by density, secondary phase, grain size and lattice defects, while the intrinsic loss is mainly caused by structure characteristics [16]. Sr_2CeO_4 samples possess high densities and no secondary phases can be detected as sintering temperature is less than 1290 °C. Considering that pure-phase Sr_2CeO_4 ceramics exhibit a uniform grain morphology and a relatively high relative density, the influence of extrinsic loss on $Q \times f$ can be thus neglected. According to the work of Kim et al. [17]. The $Q \times f$ value can be also largely dependent on the packing fraction (f) defined by summing the volume of packed ions (V_{PI}) over the volume of a primitive unit cell (V_{PUC}), as expressed by the following equation:
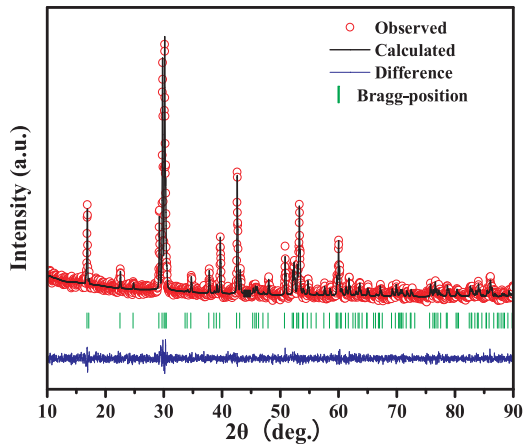
$$f(\%) = \frac{V_{PI}}{V_{PUC}} \times Z \qquad (2)$$

where Z is the number of atoms per unit cell. The calculated packing fraction values are presented in Fig. 4(b), which keeps a good consistency with the $Q \times f$ value as sintering temperature is lower than 1270 °C. $Q \times f$ values continuously increase to a maximum value of 172,600 GHz at 1270 °C, and then decrease with further increasing firing temperature. The decrease of $Q \times f$ values at higher sintering temperatures might be due to the inhomogeneous microstructure and the secondary phase as mentioned above. According to the mixing rule, we generally think that the secondary phase might not be beneficial to the $Q \times f$ value of the matrix, although microwave dielectric properties of the single-phase $SrCeO_3$ has not been reported in the literature. Moreover, it can be seen that sintering temperature exerts no apparent influence on the τ_f value and it remains around -62 ppm/°C in Fig. 4(c) since there is no obvious structure change with changing sintering temperature.
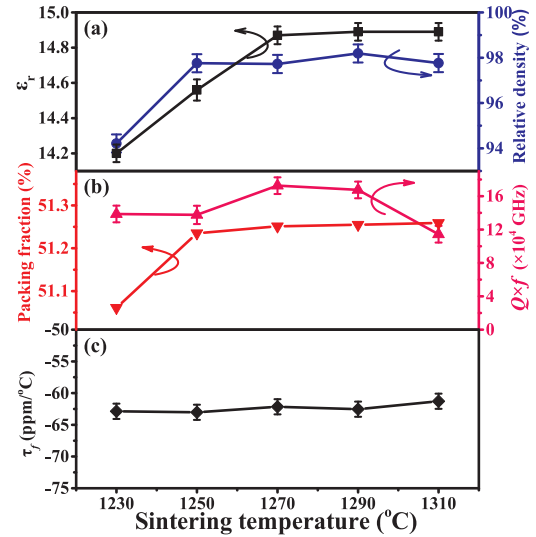
Although the Sr_2CeO_4 ceramic in present study demonstrates a high $Q \times f$ value, yet a large negative τ_f value is also accompanied. Considering that a negative τ_f value is not desirable for practical applications, a few amount of Ce^{4+} was substituted by Ti^{4+} to further tune τ_f values. Fig. 5 depicts XRD patterns of the $Sr_2Ce_{1-x}Ti_xO_4$ (0 < x ≤ 0.5) powder calcined at 1150 °C for 8 h. It is evident that a little amount of Sr_2TiO_4 phase can be observed as x ≥ 0.05, which

Fig. 1. (a) XRD patterns of Sr_2CeO_4 ceramics sintered at different temperatures for 4 h and (b) locally magnified diffraction peaks near 30°.

Table 1
Refined structural parameters, reliability factors and goodness-of-fit indicator of Sr_2CeO_4 ceramics at different sintering temperatures.

S.T. (°C)	a (Å)	b (Å)	c (Å)	Unit cell volume (Å³)	R_{wp} (%)	R_p (%)	χ^2
1230	6.1190(1)	10.3402(3)	3.5968(3)	227.78(4)	8.64	6.85	1.547
1250	6.1118(2)	10.3384(3)	3.5928(1)	227.01(2)	7.37	5.75	1.623
1270	6.1110(4)	10.3402(6)	3.5914(2)	226.94(3)	7.48	6.70	1.414
1290	6.1103(2)	10.3377(3)	3.5923(2)	226.92(2)	7.73	5.78	1.430
1310	6.1101(2)	10.3375(3)	3.5919(1)	226.90(1)	7.54	5.61	1.636

S.T: sintering temperature; R_{wp}: the reliability factor of weighted patterns; R_p: the reliability factor of patterns; χ^2: goodness-of-fit indicator $= (R_{wp}/R_{exp})^2$.

Fig. 2. Rietveld refinement plot of the Sr_2CeO_4 ceramic sintered at 1270 °C for 4 h.

Fig. 4. (a) Relative density and ε_r, (b) packing fraction and Qxf values and (c) τ_f values for Sr_2CeO_4 ceramics as a function of sintering temperature.

should be attributed to a large difference in ionic radius between Ti^{4+} and Ce^{4+}. Furthermore, the difference in crystal structure between Sr_2CeO_4 and Sr_2TiO_4 is also another important reason. The XRD patterns of $Sr_2Ce_{1-x}Ti_xO_4$ ($0 \leq x \leq 0.5$) ceramics sintered at different temperatures are shown in Fig. 6(a–c). The Sr_2CeO_4 (JCPDS No. 50-0115) and Sr_2TiO_4 (JCPDS No. 39-1471) phase can be identified as the main crystal phase for the $x \geq 0.05$ specimens, as also displayed in the calcined samples (Fig. 5). This result can be well verified by the SEM

result for the x = 0.35 sample, which exhibits two kinds of grains with different sizes in Fig. 3(d). The further EDS analysis on the large grain (marked as 1) and the small grain (marked as 2) suggests that these two kinds of grains have an approximate chemical formula of
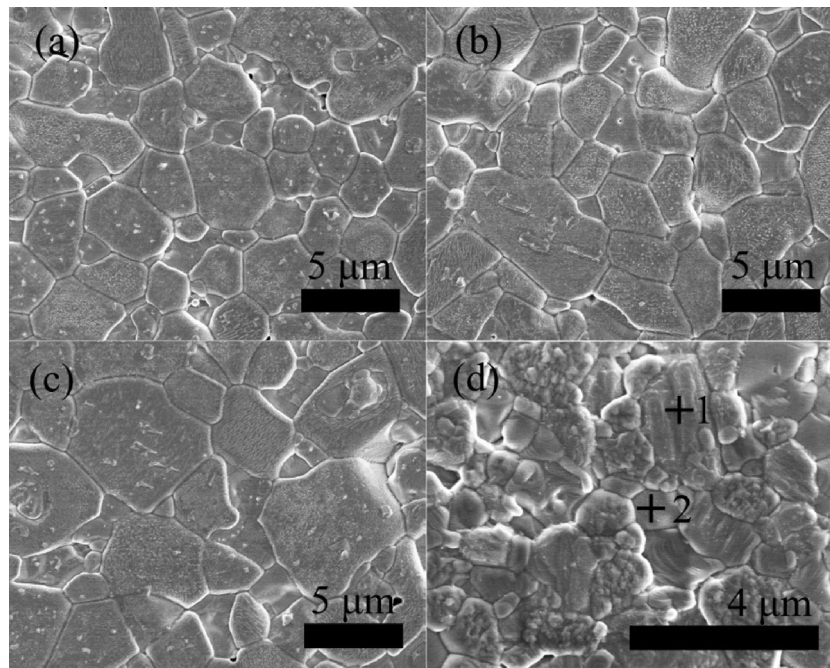
Fig. 3. SEM micrographs of Sr_2CeO_4 ceramics sintered at (a) 1270 °C, (b) 1290 °C and (c) 1310 °C, and (d) $Sr_2Ce_{0.65}Ti_{0.35}O_4$ ceramic sintered at 1350 °C.
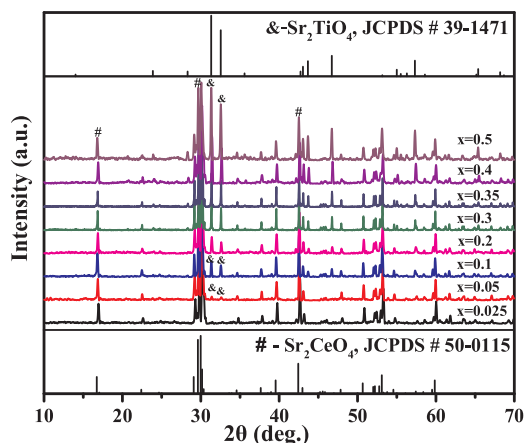
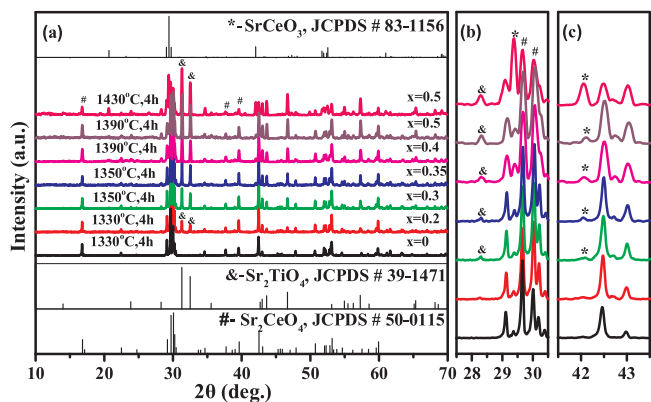**Fig. 5.** XRD patterns of $Sr_2Ce_{1-x}Ti_xO_4$ powders calcined at 1150 °C for 8 h.

Fig. 6. (a) XRD patterns of $Sr_2Ce_{1-x}Ti_xO_4$ ceramics at different sintering temperatures, (b and c) the corresponding locally-magnified diffraction peaks near 30° and 42°, respectively.

$Sr_{27.4}Ce_{14.5}O_{58.1}$ and $Sr_{30.6}Ti_{15.4}O_{54.0}$, respectively. They should correspond to the Sr_2CeO_4 phase and Sr_2TiO_4 phase, respectively. Simultaneously, the average grain size becomes obviously small compared with the x = 0 sample, indicating that the grain growth was inhibited to a certain degree. A small amount of the impurity phase $SrCeO_3$ (as marked by stars in Fig. 6(c)) was detected as sintering temperature is larger than 1350 °C. However, as sintering temperature is above 1430 °C, the amount of Sr_2CeO_4 phase is suddenly reduced, probably because of its decomposition into $SrCeO_3$ [18]. The corresponding sample was then composed of the dominant $SrCeO_3$, Sr_2TiO_4 phases and the residual Sr_2CeO_4 phase. The amount of the impurity phase $SrCeO_3$ almost unchanges as sintering temperature is lower than 1430 °C. It means that Sr_2CeO_4 decomposes readily into $SrCeO_3$ at 1430 °C in air. As a result, the substitution of Ti^{4+} for Ce^{4+} can lead to the appearance of Sr_2TiO_4. Meanwhile, the diffraction peak intensity of the Sr_2TiO_4 phase was found to increase with an increment of x.

The obvious difference in their structures would determine the possibility of stable coexistence of Sr_2TiO_4 and Sr_2CeO_4 phases in the sintered bodies within a certain temperature. Fig. 7 shows the variation of relative density and ε_r of $Sr_2Ce_{1-x}Ti_xO_4$ ceramics as a function of sintering temperature. It can be seen that the optimum sintering temperature of each sample increases with increasing x. With an increase of sintering temperature, the relative density of each composition firstly increases to a maximum value, and then decreases slightly with further increasing sintering temperature (see in Fig. 7(a)). ε_r generally increases with increasing sintering temperature, as shown in Fig. 7(b). For x > 0.35, as sintering temperature is lower than 1410 °C, it could be ascribed to the improvement of sample density. With further increasing
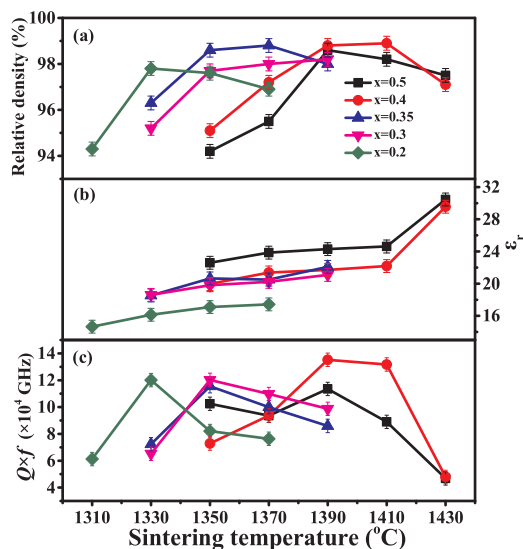

Fig. 7. The variation of (a) relative density, (b) ε_r and (c) Qxf values for $Sr_2Ce_{1-x}Ti_xO_4$ ceramics as a function of sintering temperature.

temperature, a rapid increase of ε_r probably due to the appearance of the $SrCeO_3$ phase. Fig. 7(c) shows the variation of $Q \times f$ for $Sr_2Ce_{1-x}Ti_xO_4$ ceramics as a function of sintering temperature. The same variation trend in $Q \times f$ and relative density with sintering temperature indicates that density acts as a main controlling factor of dielectric loss. The decomposition of Sr_2CeO_4 phase can be also used to explain the deterioration of $Q \times f$, as sintering temperature is close to 1430 °C.

Microwave dielectric properties of $Sr_2Ce_{1-x}Ti_xO_4$ (x = 0-0.5) ceramics sintered at optimum temperatures are shown in Fig. 8. It can be seen that ε_r increases monotonously from 14.9 at x = 0 to 24.3 at x = 0.5. The ε_r value was increased because of a relatively high ε_r value of the Sr_2TiO_4 ceramic compared with that of the Sr_2CeO_4 ceramic [14]. $Q \times f$ decreases firstly with increasing x, and then almost keeps nearly constant within the studied composition range. The decrease of $Q \times f$ values for $Sr_2Ce_{1-x}Ti_xO_4$ ceramics might be due to a relatively low $Q \times f$ value of the Sr_2TiO_4 phase [14]. In addition, it might be also ascribed to the fact that the distribution of two phases is not perfectly uniform in the sintered ceramic body. The microwave dielectric properties of these two phases in the composite ceramic might be different from those in their respective monophasic ceramics owing to the ionic inter-diffusion during sintering [19]. τ_f exhibits an approximately linear change from large negative values to positive values with increasing x owing to a large positive τ_f value of Sr_2TiO_4 [14], which is in good agreement with
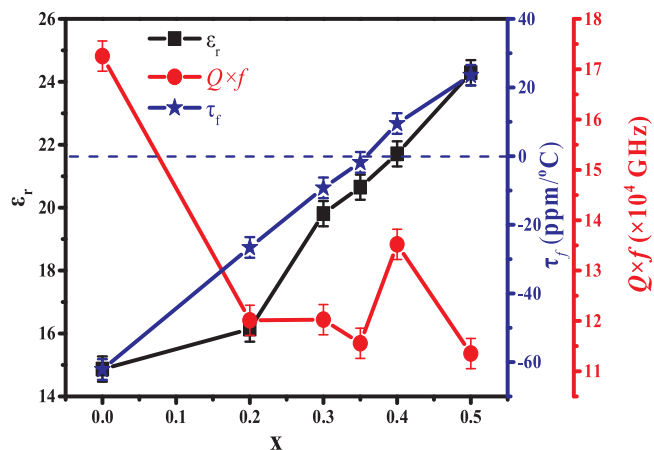

Fig. 8. Microwave dielectric properties of $Sr_2Ce_{1-x}Ti_xO_4$ ceramics sintered at optimum temperatures.

an empirical model for multiphase ceramics [20,21]. As a result, near-zero τ_f values can be obtained approximately near x = 0.35. The optimal microwave dielectric properties of ε_r = 20.7, $Q \times f$ = 115,550 GHz and τ_f = -1.8 ppm/°C are obtained for the x = 0.35 ceramic, showing good application potentials.

4. Conclusions

In this work, a novel low-loss Sr_2CeO_4 microwave dielectric ceramic with a one-dimensional chain structure was successfully prepared by a standard solid-state reaction method. The compound with homogeneous and dense microstructure exhibits an ε_r of 14.8, and ultra-high $Q \times f$ of 172,600 GHz (9.4 GHz), and a τ_f of -62 ppm/°C as sintered at 1270 °C for 4 h. Moreover, the substitution of Ti^{4+} for Ce^{4+} in Sr_2CeO_4 ceramics was found to induce the Sr_2TiO_4 phase, leading to an obvious change of τ_f from negative to positive values. Meanwhile, the ε_r value of the ceramics gradually increases, while the $Q \times f$ values decrease slightly. The optimum microwave dielectric properties of ε_r = 20.7, $Q \times f$ = 115,550 GHz (8.1 GHz) and τ_f = -1.8 ppm/°C are obtained in the x = 0.35 composition as sintered at 1350 °C for 4 h.

Acknowledgement

References

[1] T.A. Vanderah, Talking ceramics, Science 298 (2002) 1182–1184.
[2] I.M. Reaney, D. Iddles, Microwave dielectric ceramics for resonators and filters in mobile phone networks, J. Am. Ceram. Soc. 89 (2006) 2063–2072.
[3] M.T. Sebastian, R. Ubic, H. Jantunen, Low-loss dielectric ceramic materials and their properties, Int. Mater. Rev. 60 (2015) 392–412.
[4] F. Zhao, Z.X. Yue, J. Pei, Z.L. Gui, L.T. Li, Effects of octahedral thickness variance on the temperature coefficient of resonant frequency of the B-site deficient hexagonal perovskites, Appl. Phys. Lett. 90 (2007) 142908.
[5] A. Kan, H. Ogawa, K. Mori, H. Ohsato, Y. Andou, Chemical bonding characteristics and dielectric properties of $Nd_2(Ba_{1-x}Sr_x)ZnO_5$ solid solutions, J. Mater. Res. 18 (2003) 2427–2434.
[6] Y.Y. Zhou, S.Q. Meng, H.C. Wu, Z.X. Yue, Microwave dielectric properties of $Ba_2Ca_{1-x}Sr_xWO_6$ double perovskites, J. Am. Ceram. Soc. 94 (2011) 2933–2938.
[7] E.S. Kim, S.H. Kim, B.I. Lee, Low-temperature sintering and microwave dielectric properties of $CaWO_4$ ceramics for LTCC applications, J. Eur. Ceram. Soc. 26 (2006) 2101–2104.
[8] H. Zhuang, Z.X. Yue, F. Zhao, J. Pei, L.T. Li, Microstructure and microwave dielectric properties of $Ba_5Nb_4O_{15}$-$BaWO_4$ composite ceramics, J. Alloys Compd. 472 (2009) 411–415.
[9] D. Zhou, L.X. Pang, J. Guo, Z.M. Qi, T. Shao, Q.P. Wang, H.D. Xie, X. Yao, C.A. Randall, Influence of Ce substitution for Bi in $BiVO_4$ and the impact on the phase evolution and microwave dielectric properties, Inorg. Chem. 53 (2014) 1048–1055.
[10] E. Danielson, M. Devenney, D.M. Giaquinta, J.H. Golden, R.C. Haushalter, E.W. Mcfarland, D.M. Poojary, C.M. Reaves, W.H. Weinberg, X.D. Wu, A rare-earth phosphor containing one-dimensional chains identified through combinatorial methods, Science 279 (1998) 837–839.
[11] S.N. Ruddlesden, P. Popper, The compound $Sr_3Ti_2O_7$ and its structure, Acta Cryst. 11 (1958) 54–55.
[12] E. Danielson, M. Devenney, D.M. Giaquinta, J.H. Golden, R.S. Haushalter, E.W. McFarland, D.M. Poojary, C.M. Reaves, W.H. Weinberg, X.D. Wu, X-ray powder structure of Sr_2CeO_4: a new luminescent material discovered by combinatorial chemistry, J. Mol. Struct. 470 (1998) 229–235.
[13] R.G. Gerlach, S.S. Bhella, V. Thangadurai, Facile conversion of layered ruddlesden-ropper-related structure Y_2O_3-doped Sr_2CeO_4 into fast oxide ion-conducting fluorite-type Y_2O_3-doped CeO_2, Inorg. Chem. 48 (2009) 257–266.
[14] B. Liu, L. Li, X.Q. Liu, X.M. Chen, $Sr_{n+1}TinO_{3n+1}$ (n = 1, 2) microwave dielectric ceramics with medium dielectric constant and ultra-low dielectric loss, J. Am. Ceram. Soc. 100 (2017) 496–500.
[15] T. Grzyb, A. Szczeszak, J. Rozowska, J. Legendziewicz, S. Lis, Tunable luminescence of Sr_2CeO_4: M^{2+} (M = Ca, Mg, Ba, Zn) and Sr_2CeO_4: Ln^{3+} (Ln = Eu, Dy, Tm) nanophosphors, J. Phys. Chem. C 116 (2012) 3219–3226.
[16] Y.C. Chen, Y.N. Wang, C.H. Hsu, Enhancement microwave dielectric properties of Mg_2SnO_4 ceramics by substituting Mg^{2+} with Ni^{2+}, Mater. Chem. Phys. 133 (2012) 829–833.
[17] E.S. Kim, B.S. Chun, R. Freer, R.J. Cernik, Effects of packing fraction and bond valence on microwave dielectric properties of $A^{2+}B^{6+}O_4$ (A^{2+}: Ca, Pb, Ba; B^{6+}: Mo, W) ceramics, J. Eur. Ceram. Soc. 30 (2010) 1731–1736.
[18] W.H. Kan, V. Thangadurai, Thermochemistry of $Sr_2Ce_{1-x}Pr_xO_4$ (x = 0, 0.2, 0.5, 0.8, and 1): variable-temperature and –atmosphere in-situ and ex-situ powder X-ray diffraction studies and their physical properties, Inorg. Chem. 51 (2012) 8973–8981.
[19] M.Z. Dong, Z.X. Yue, H. Zhuang, S.Q. Meng, L.T. Li, Microstructure and microwave dielectric properties of TiO_2-doped Zn_2SiO_4 ceramics synthesized through the sol-gel process, J. Am. Ceram. Soc. 91 (2008) 3981–3985.
[20] D.W. Kim, B. Park, J.H. Chung, K.S. Hong, Mixture behavior and microwave dielectric properties in the low-fired TiO_2-CuO system, J. Appl. Phys. 39 (2000) 2696–2700.
[21] S.H. Yoon, G.K. Choi, D.W. Kim, S.Y. Cho, K.S. Hong, Mixture behavior and microwave dielectric properties of (1-x)$CaWO_4$-$xTiO_2$, J. Eur. Ceram. Soc. 27 (2007) 3087–3091.